Computation of Cavity Resonances Using Edge-Based Finite Elements

A. Chatterjee, J. M. Jin, and J. L. Volakis

Abstract—**In this paper, the eigenvalues of a cavity resonator are computed using edge-based finite elements, and it is shown that these elements offer significant improvements in accuracy, in addition to being suitable for modelling arbitrarily shaped inhomogeneous regions. A performance comparison between the edge-based tetrahedra and rectangular brick elements is also carried out.**

I. Introduction

Solving Maxwell's equations for the resonances of a closed cavity is important in understanding and controlling the operation of many devices, including particle accelerators, microwave filters, microwave ovens and optical fibers. However, the exact eigenvalues can be obtained only for simple geometries. For arbitrarily shaped cavities, numerical techniques like the finite element method must be used, but the occurrence of "spurious" modes [1] in the node-based finite element approach has plagued the computation of their eigenvalues. This difficulty can be circumvented with the introduction of a penalty term [2] to render the finite element vector field solutions nondivergent. However, it is difficult to satisfy continuity requirements across material interfaces and treat geometries with sharp edges [3] using classical finite-elements, obtained by interpolating the nodal values of the vector field components. Edge elements, a type of vector finite elements with their degrees of freedom associated with the edges of the mesh, have been shown to be free of these shortcomings [4]–[6]. Edge-based finite elements are, therefore, a natural choice for treating three dimensional geometries. Generally these lead to more unknowns but the higher variable count is balanced by the greater sparsity of the finite element matrix so that the computation time required to solve such a system iteratively with a given accuracy is less than the traditional approach [7].

In this paper, we have solved for the eigenvalues of an arbitrarily shaped metallic cavity using node-based and edge-based vector finite elements. The computed data are then compared with analytical results for empty and partially filled cavities. A comparison between the storage intensity and computational accuracy for edge-based rectangular bricks and tetrahedra is also presented. Finally, we compute the eigenvalues of a metallic cavity with a ridge along one of its faces.

II. Formulation

2.1 Finite Element Equations

Consider a three dimensional inhomogeneous body occupying the volume V. To discretize the electric field E within this volume, we subdivide the volume into small tetrahedra or rectangular bricks, each occupying the volume V_e ($e = 1, 2, \cdots, M$), where M is the total number of elements. For a numerical solution of $\boldsymbol{E}$, we expand it within the eth volume element as

$$\boldsymbol{E} = \sum_{j=1}^{m} E_j^e \, \boldsymbol{W}_j^e \tag{1}$$

where $\boldsymbol{W}_j^e$ are the edge-based vector basis functions, E_j^e denote the expansion coefficients of the basis, m represents the number of edges comprising the element and the superscript stands for the element number. On substituting this into the usual vector wave equation and upon applying Galerkin's technique, some vector identities and the divergence theorem, we obtain the weak form of Maxwell's equation:

$$R_i^e = \sum_{j=1}^{m} E_j^e \int_{V_e} \left[\frac{1}{\mu_r} (\nabla \times \boldsymbol{W}_i^e) \cdot (\nabla \times \boldsymbol{W}_j^e) - k_0^2 \epsilon_r \boldsymbol{W}_i^e \cdot \boldsymbol{W}_j^e \right] dv - jk_0 Z_0 \oint_{S_e} \boldsymbol{W}_i^e \cdot (\hat{\boldsymbol{n}} \times \boldsymbol{H}) \, ds \tag{2}$$

where R_i^e represents the weighted residual integral for element e, S_e denotes the surface enclosing V_e, $\hat{\boldsymbol{n}}$ is the outward unit vector normal to S_e, Z_o is the free-space intrinsic impedance and ϵ_r, μ_r is the material permittivity and permeability, respectively. Equation (2) can be conveniently written in matrix form as

$$\{R_i^e\} = [A^e]\{E^e\} - k_0^2 [B^e]\{E^e\} - \{C^e\} \tag{3}$$

where

$$A_{ij}^e = \int_{V_e} \frac{1}{\mu_r} (\nabla \times \boldsymbol{W}_i^e) \cdot (\nabla \times \boldsymbol{W}_j^e) \, dv \tag{4}$$

$$B_{ij}^e = \int_{V_e} \epsilon_r \boldsymbol{W}_i^e \cdot \boldsymbol{W}_j^e \, dv \tag{5}$$

$$C_i^e = jk_0 Z_0 \oint_{S_e} \boldsymbol{W}_i^e \cdot (\hat{\boldsymbol{n}} \times \boldsymbol{H}) \, ds \tag{6}$$

and on assembling the equations from all the elements making up the geometry, we obtain the system

$$\sum_{e=1}^{M} \{R_i^e\} = \sum_{e=1}^{M} [A^e]\{E^e\} - k_0^2 \sum_{e=1}^{M} [B^e]\{E^e\} - \sum_{e=1}^{M} \{C^e\} = \{0\} \tag{7}$$

where all matrices and vectors following the summation sign have been augmented using global numbers.

Due to the continuity of tangential $\boldsymbol{H}$ at the interface between two dielectrics, an element face lying inside the body does not contribute to the last term of (7) in the final assembly of the element equations. As a result, the last term of (7) reduces to a column vector containing the surface integral of the tangential magnetic field only over the outer surface of the body. In this application, the surface enclosing the volume of the body V is perfectly conducting and, thus, the coefficients associated with the edges bordering the perfectly conducting surface can be set to zero a priori. This reduces the original unknown count and eliminates the need to generate equations for those edges/unknowns which would have otherwise involved the column vector $\{C^e\}$. Also since $\{C^e\}$ is only associated with boundary edges, the surface integral associated with it vanishes and (7) can be written as

$$[A]\{E\} = \lambda [B]\{E\} \tag{8}$$

where $[A]$ and $[B]$ are $N \times N$ symmetric, sparse matrices with N being the total number of edges resulting from the subdivision of the body excluding the edges on the boundary, $\{E\}$ is a $N \times 1$ column vector denoting the edge fields and $\lambda = k_0^2$ gives the eigenvalues of the system. A solution of (8) will yield the resonant field distribution $\{E\}$ and the corresponding wavenumber k_0.

Manuscript received August 13, 1991; revised April 10, 1992.

The authors are with the Department of Electrical Engineering and Computer Science, University of Michigan, Ann Arbor, MI 48109-2122.

IEEE Log Number 9202905.

TABLE I
TETRAHEDRON EDGE DEFINITION

Edge No.	i_1	i_2
1	1	2
2	1	3
3	1	4
4	2	3
5	4	2
6	3	4

2.2 *Basis Functions*

The vector edge-based expansion functions for rectangular bricks were presented in [8]. Vector fields within tetrahedral domains can be conveniently represented by expansion functions that are linear in the spatial variables and have either zero divergence or zero curl. The basis functions defined in [7] are associated with the six edges of the tetrahedron and have zero divergence and constant curl. To define them, let us assume that i_1 and i_2 are the terminal nodes of the ith edge and the six edges of a tetrahedron are numbered according to Table I. The vector basis function associated with the $(7 - i)$th edge of the tetrahedron is then given by

$$\boldsymbol{W}^e_{7-i} = \begin{cases} \boldsymbol{f}_{7-i} + \boldsymbol{g}_{7-i} \times \boldsymbol{r}, & \boldsymbol{r} \text{ in the tetrahedron} \\ 0, & \text{otherwise} \end{cases} \tag{9}$$

with

$$\boldsymbol{f}_{7-i} = \frac{b_{7-i}}{6V_e} \boldsymbol{r}_{i_1} \times \boldsymbol{r}_{i_2} \tag{10}$$

$$\boldsymbol{g}_{7-i} = \frac{b_i b_{7-i} \boldsymbol{e}_i}{6V_e} \tag{11}$$

in which $i = 1, 2, \cdots, 6$, V_e is the volume of the tetrahedral element, $\boldsymbol{e}_i = (\boldsymbol{r}_{i_2} - \boldsymbol{r}_{i_1})/b_i$ is the unit vector of the ith edge and $b_i = |\boldsymbol{r}_{i_2} - \boldsymbol{r}_{i_1}|$ is the length of the ith edge with $\boldsymbol{r}_{i_1}$ and $\boldsymbol{r}_{i_2}$ denoting the location of the i_1 and i_2 nodes.

In general, the implementation of the above discretization will involve two numbering systems, and thus some unique global edge direction must be defined to ensure the continuity of $\hat{\boldsymbol{n}} \times \boldsymbol{E}$ across all edges [9]. Here we choose this direction to be coincident with the edge vector pointing from the smaller to the larger global node number. Finally, since $\nabla \cdot \boldsymbol{W}^e_i = 0$, the electric field obtained from a solution of (3) satisfies the divergence equation within each element and, thus, the solution will be free from contamination due to spurious solutions.

III. RESULTS

In Table II, we present a comparison of the percentage error in the computation of eigenvalues for a 1 cm × .5 cm × .75 cm rectangular cavity using edge-based rectangular bricks and tetrahedra. The edge-based approach using tetrahedral elements predicts the first six distinct non-trivial eigenvalues with less than 4 percent error and is seen to provide better accuracy than rectangular brick elements. The maximum edge length for the rectangular brick elements was .15 cm whereas that for the tetrahedral elements was .2 cm. To investigate this matter further, we consider a cubical metallic cavity having a side length of .5 cm. A plot of the percentage error in calculating the first three degenerate resonant frequencies versus the number of unknowns is given in Fig. 1 for both rectangular bricks and tetrahedral elements. It is clear in this example that the tetrahedral elements predict the eigenvalues with greater accuracy than the rectangular bricks.

TABLE II
EIGENVALUES (k_0, cm^{-1}) FOR AN EMPTY 1 cm × 0.5 cm × 0.75 cm RECTANGULAR CAVITY

Mode	Analytical	Computed (bricks) 270 Unknowns	Computed (tetra.) 260 Unknowns	Error (%) (bricks)	Error (%) (tetra.)
TE_{101}	5.236	5.307	5.213	−1.36	.44
TM_{110}	7.025	7.182	6.977	−2.23	.70
TE_{011}	7.531	7.725	7.474	−2.58	1.00
TE_{201}		7.767	7.573	−3.13	−.56
TM_{111}	8.179	8.350	7.991	−2.09	2.29
TE_{111}		8.350	8.122	−2.09	.70
TM_{210}	8.886	9.151	8.572	−2.98	3.53
TE_{102}	8.947	9.428	8.795	−5.38	1.70

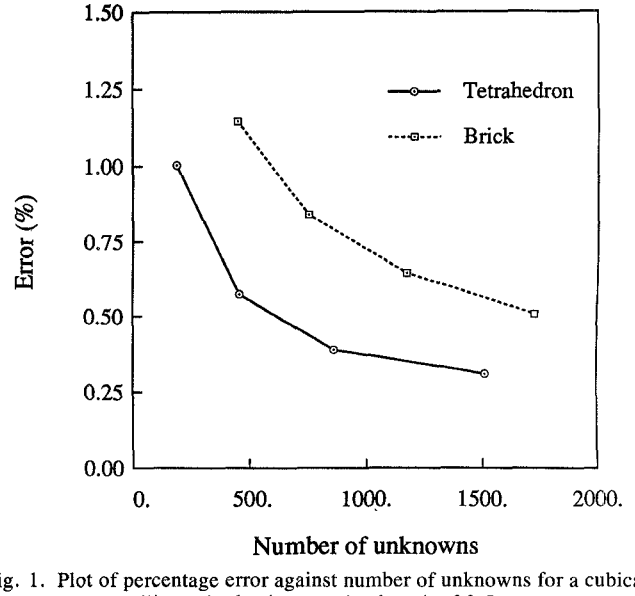

Fig. 1. Plot of percentage error against number of unknowns for a cubical metallic cavity having an edge length of 0.5 cm.

TABLE III
EIGENVALUES (k_0, cm^{-1}) FOR A HALF-FILLED 1 cm × 0.1 cm × 1 cm RECTANGULAR CAVITY HAVING A DIELECTRIC FILLING OF $\epsilon_r = 2$ EXTENDING FROM $z = 0.5$ cm to $z = 1.0$ cm

Mode	Analytical	Computed 192 Unknowns	Error (%)
TEz_{101}	3.538	3.534	.11
TEz_{201}	5.445	5.440	.10
TEz_{102}	5.935	5.916	.32
TEz_{301}	7.503	7.501	.04
TEz_{202}	7.633	7.560	.97
TEz_{103}	8.096	8.056	.50

In Tables III and IV, we compare the exact eigenvalues with those computed using edge-based tetrahedral finite elements. The finite element mesh was generated using SDRC I-DEAS, a commercial pre-processing package, and it is seen that the numerical results are in good agreement with the exact values for both homogeneous and inhomogeneous cavities. The exact eigenvalues of the half-filled cavity as described in Table III are computed by solving the transcendental equation obtained upon matching the tangential electric and magnetic fields at the air-dielectric interface. As seen, these results agree with those predicted by the finite ele-

TABLE IV
EIGENVALUES (k_0, cm^{-1}) FOR AN EMPTY SPHERICAL CAVITY OF RADIUS 1 cm

Mode	Analytical	Computed 300 Unknowns	Error (%)
TM_{010}	2.744	2.799	−2.04
$TM_{111,even}$		2.802	−2.11
$TM_{111,odd}$		2.811	−2.44
TM_{021}	3.870	3.948	−2.02
$TM_{121,even}$		3.986	−2.99
$TM_{121,odd}$		3.994	−3.20
$TM_{221,even}$		4.038	−4.34
$TM_{221,odd}$		4.048	−4.59
TE_{011}	4.493	4.433	1.33
$TE_{111,even}$		4.472	.47
$TE_{111,odd}$		4.549	−1.25

TABLE V
TEN LOWEST NON-TRIVIAL EIGENVALUES (k_0, cm^{-1}) FOR THE GEOMETRY DRAWN IN FIG 2: (a) 267 UNKNOWNS; (b) 671 UNKNOWNS

No.	(a)	(b)
1	4.941	4.999
2	7.284	7.354
3	7.691	7.832
4	7.855	7.942
5	8.016	7.959
6	8.593	8.650
7	8.906	8.916
8	9.163	9.103
9	9.679	9.757
10	9.837	9.927

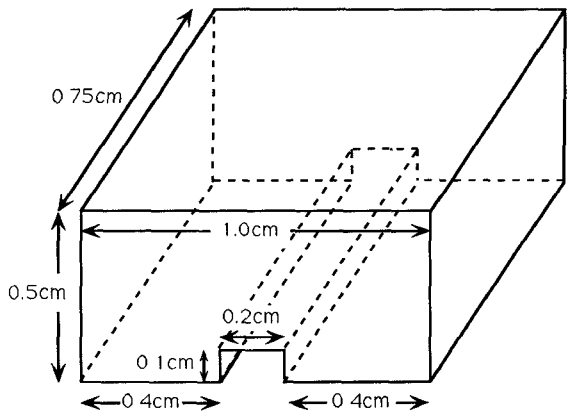

Fig. 2. Geometry for Table V.

ment solution to within 1 percent (no symmetry was assumed in this solution). Similar comparisons are given in Table IV for a sphere having 1 cm radius. Finally, Table V presents the eigenvalues of the geometry illustrated in Fig. 2. This is a closed metallic cavity with a ridge along one of its faces.

It is noted that as the degeneracy of the eigenvalues increases, the matrix becomes increasingly ill-conditioned and the numerical solution is correspondingly less accurate [10]. This is clearly observed from the data in Table IV for the case of a perfectly conducting hollow spherical cavity. Since the second lowest TM mode has five-fold degeneracy, the computational error is seen to be the greatest. However, for the partially filled rectangular cavity, the absence of degenerate modes gives results which are accurate to within 1 percent of the exact eigensolutions. We finally remark of the inherent presence of zero eigenvalues in our computations whose number is equal to the internal nodes. These zero eigenvalues are easily identifiable and since they do not correspond to physical modes, they were always discarded.

IV. CONCLUSIONS

It was shown that the resonant frequencies of an arbitrarily shaped inhomogeneously filled metallic resonator can be computed very accurately via the finite element method using edge-based tetrahedral elements. The same method in conjunction with node-based elements is much less reliable and not readily applicable to regions containing discontinuous boundaries in shape and material. Edge-based rectangular bricks do not provide as good an accuracy as edge-based tetrahedral elements and their use is further limited to a special class of geometries.

REFERENCES

[1] Z. J. Cendes and P. Silvester, "Numerical solution of dielectric loaded waveguides: I—Finite element analysis," *IEEE Trans. Microwave Theory Tech.*, vol. 18, pp. 1124–1131, 1970.
[2] B. M. A. Rahman and J. B. Davies, "Penalty function improvement of waveguide solution by finite elements," *IEEE Trans. Microwave Theory Tech.*, vol. 32, pp. 922–928, Aug. 1984.
[3] J. P. Webb, "Finite element analysis of dispersion in waveguides with sharp metal edges," *IEEE Trans. Microwave Theory Tech.*, vol. 36, no. 12, pp. 1819–1824, Dec. 1988.
[4] A. Bossavit, "A rationale for 'edge-elements' in 3-D fields computations," *IEEE Trans. Magn.*, vol. 24, no. 1, pp. 74–79, Jan. 1988.
[5] J. Wang and N. Ida, "Eigenvalue analysis in EM cavities using divergence free finite elements," *IEEE Trans. Magn.*, vol. 27, no. 5, pp. 3978–3981, Sept. 1991.
[6] K. Sakiyama, H. Kotera, and A. Ahagon, "3-D electromagnetic field mode analysis using finite element method by edge element," *IEEE Trans. Magn.*, vol. 26, no. 5, pp. 1759–1761, Sept. 1990.
[7] M. L. Barton and Z. J. Cendes, "New vector finite elements for three-dimensional magnetic field computation," *J. Appl. Phys.*, vol. 61, no. 8, pp. 3919–3921, Apr. 1987.
[8] J. M. Jin and J. L. Volakis, "Electromagnetic scattering by and transmission through a three-dimensional slot in a thick conducting plane," *IEEE Trans. Antennas Propagat.*, vol. 39, no. 4, pp. 543–550, Apr. 1991.
[9] X. Yuan, "Three-dimensional electromagnetic scattering from inhomogeneous objects by the hybrid moment and finite element method," *IEEE Trans. Microwave Theory Tech.*, vol. 38, no. 8, pp. 1053–1059, Aug. 1990.
[10] G. H. Golub and C. F. Van Loan, *Matrix Computations*. Baltimore: The Johns Hopkins University Press, 1985, pp. 202–204.

Dielectric Property Measurements of Materials Using the Cavity Technique

Ahmet Baysar and James L. Kuester

***Abstract*—A cavity technique based on frequency shift was used to measure dielectric properties (dielectric constant and loss factor) of some particulate materials as a function of temperature. The materials studied were alumina, cobalt/alumina, dolomite and sand. The prop-**

Manuscript received October 28, 1991; revised April 22, 1992.
The authors are with the Department of Chemical, Bio and Materials Engineering, Arizona State University, Tempe, AZ 85287.
IEEE Log Number 9202906.